

## Formation of Electrostatic Potential Barrier between Different Plasmas

R. Hatakeyama, Y. Suzuki, and N. Sato

*Department of Electronic Engineering, Tohoku University, 980 Sendai, Japan*

(Received 28 October 1982)

A potential depression is formed between two magnetized plasmas with different electron temperatures and ion species in the absence of electric current passing through them. The depression is deep enough to reflect both groups of electrons, reducing thermal contact between the plasmas. By addition of a magnetic bump to a uniform magnetic field, the potential dip is localized around the mirror point. A dependence of the phenomenon on neutral-gas pressure is also clarified.

PACS numbers: 52.25.Fi, 52.55.Ke, 52.75.Ds

There has been an increasing interest in electrostatic potential formations along a magnetic field in conjunction with auroral particles<sup>1</sup> in space plasma and plasma confinement in open-ended fusion devices.<sup>2</sup> In a tandem-mirror system where a fusion plasma is expected to be confined in a central cell between end-plug mirror cells,<sup>2</sup> it is of crucial importance to know how to form a necessary potential configuration. In the TMX and Phaedrus experiments, the end loss of central-cell ions was reduced by the tandem potential.<sup>3</sup> To improve the reactor picture, however, there are advantages to having hot electrons in the end plugs.<sup>4</sup> As a possibility for maintaining two plasmas with different electron temperatures in two spatially separated regions, it has been proposed to form a potential depression between the two regions, which isolates the two groups of electrons from each other, acting as a thermal barrier.<sup>4</sup> As far as the auroral-particle acceleration is concerned, it is important to know the potential configuration in a contact region between a hot magnetospheric plasma and a cold ionospheric plasma.<sup>5</sup>

Here a potential depression is experimentally demonstrated to be formed between two plasmas with different electron temperatures and ion species. The result is obtained in the absence of any externally applied potential difference between (and electric current through) the plasmas. In this sense, the phenomenon is related to electric double layers without current in plasmas,<sup>6</sup> which cannot be realized in the works<sup>7,8</sup> on double layers with external voltage and/or current sources.

Two different plasmas are produced, respectively, at two ends in a straight 15.7-cm-diam stainless-steel vacuum chamber, as shown in Fig. 1. A Q-machine plasma<sup>8</sup> with density  $N_1$  ( $\approx 3 \times 10^9 \text{ cm}^{-3}$ ), electron and ion temperatures  $T_{e10}$  and  $T_{i10}$  ( $\approx T_{e10} \approx 0.2 \text{ eV}$ ), is produced by

contact ionization of potassium atoms at a hot tantalum plate [source 1 ( $S_1$ )] under the electron-rich condition. The other plasma with density  $N_2$  ( $10^8$ – $10^9 \text{ cm}^{-3}$ ) is produced by an argon-gas discharge between mesh anode  $A$  and oxide cathode  $K$  [source 2 ( $S_2$ )] (the maintaining voltage between  $A$  and  $K$  is around 15 V). The separation between  $S_1$  and  $S_2$  is 200–300 cm. The argon gas is fed near  $K$  by keeping the gas pressure near  $S_2$  in the range  $1.5 \times 10^{-4}$ – $1.5 \times 10^{-3}$  Torr. A differential pumping yields the pressure of  $4.0 \times 10^{-5}$ – $8.0 \times 10^{-4}$  Torr in the experimental region. The electron temperature of the discharge plasma,  $T_{e20}$  ( $\approx 2.0 \text{ eV}$ ), is larger than  $T_{e10}$  by an order of magnitude, although the ion temperature  $T_{i20}$  is nearly equal to  $T_{i10}$ . The two plasmas of about 3.5 cm in diameter diffuse along a strong magnetic field  $B$  (1–4 kG) in opposite directions. Their plasma pressures near the sources are defined by  $P_{10} = N_1 T_{10}$  [ $= N_1 (T_{e10} + T_{i10})$ ] and  $P_{20} = N_2 T_{20}$  [ $= N_2 (T_{e20} + T_{i20})$ ] while their local pressures are defined by  $P_1 = n_1 T_1$  [ $= n_1 (T_{e1} + T_{i1})$ ] and  $P_2 = n_2 T_2$  [ $= n_2 (T_{e2} + T_{i2})$ ], respectively.  $A$  is grounded electrically together with the vacuum

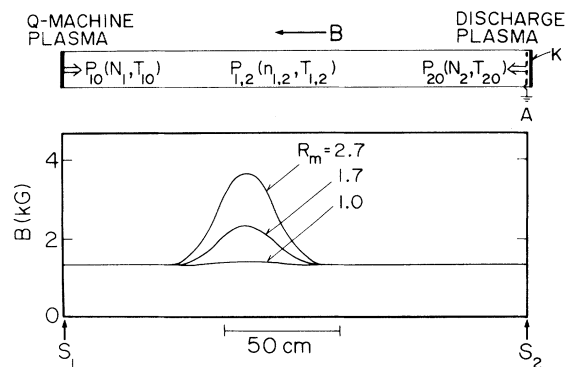


FIG. 1. Schematic of experimental device with two different plasma sources ( $S_1, S_2$ ) and magnetic-field configuration  $B$ .

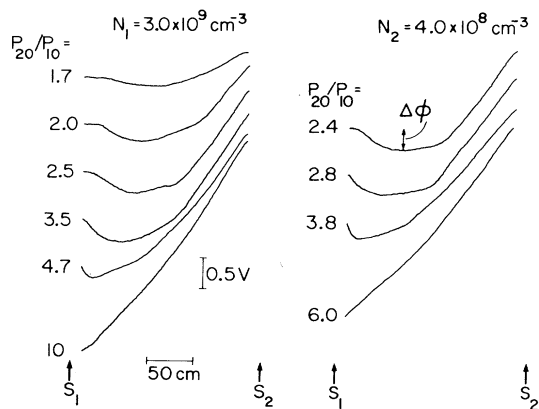


FIG. 2. Potential distributions along the plasma column for various ratios of the plasma pressures,  $P_{20}/P_{10}$ , at the sources with  $N_1$  or  $N_2$  kept constant under the uniform magnetic field. The argon-gas pressure is  $2 \times 10^{-4}$  Torr in the experimental region ( $8 \times 10^{-4}$  Torr near  $S_2$ ). The curves are shifted vertically one after another (the potential near  $S_2$  is almost independent of  $P_{20}/P_{10}$ ).

chamber to fix the potential of the discharge plasma.  $S_1$  is kept at floating potential (there is no externally applied potential difference between  $S_1$  and  $S_2$ ). There is no net electric current along the plasma column. A local magnetic bump with mirror ratio  $R_m$  ( $\approx 3.0$ ) can be produced between  $S_1$  and  $S_2$ , as shown also in Fig. 1. The ion Larmor radius ( $\approx 0.3$  cm) is much smaller than the plasma radius. The collision mean free paths between charged particles are longer than 50 cm. According to Brown's data book,<sup>9</sup> the mean free path of electrons is in the range 60–1200 cm while that of ions with neutral particles (including charge-exchange collisions) is in the range 10–200 cm under our conditions. The plasma potential  $\phi$  is determined by axially movable emissive probes (spatial resolution  $\approx 1$  mm) and is checked by the Langmuir probe method.

First of all, measurements are performed on  $\phi$  along the uniform magnetic field ( $R_m = 1$ ). When we have only the discharge plasma ( $S_1$  is not heated), a monotonic decrease of  $\phi$  towards  $S_1$  is observed, as expected from ambipolar diffusion along the magnetic field. When  $S_1$  is heated hot enough for plasma production, however, we can recognize an increase of  $\phi$  near  $S_1$ . With an increase of plasma supply from  $S_1$ , a spatial region of this potential increase spreads towards  $S_2$  and there appears a broad potential minimum along the plasma column. The position of this potential dip is controlled by changing the pres-

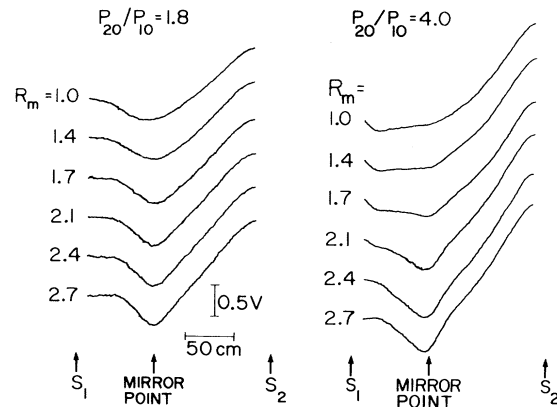


FIG. 3. Potential distributions in the presence of the magnetic bump with mirror ratio  $R_m$  at typical plasma-pressure ratios  $P_{20}/P_{10} = 1.8$  and  $4.0$ . The argon-gas pressure is  $2 \times 10^{-4}$  Torr ( $8 \times 10^{-4}$  Torr near  $S_2$ ).

sure ratio  $P_{20}/P_{10}$ , as presented in Fig. 2. The dip shifts towards  $S_1$  when  $N_2$  is increased with  $N_1$  kept constant. The shift towards  $S_1$  is also observed when  $N_1$  is decreased with  $N_2$  kept constant. The results imply that there might be a plasma-pressure balance between the two plasmas at the position where the negative dip is formed. By operation of only  $S_1$  ( $S_2$ ), the local plasma pressure  $P_1$  ( $P_2$ ) is measured at the position where the potential minimum could be observed under the operation of both  $S_1$  and  $S_2$ . The measurements show that  $P_2/P_1$  is approximately unity around the dip position. The depression depth is on the order of  $T_{e1}/e$  which is large enough to reflect most electrons supplied from  $S_1$ .

When a local magnetic bump is added to the uniform field, a potential change due to the magnetic mirror is observed near the mirror point even in the case of the monotonic potential variation under the uniform magnetic field. This change is enhanced under the condition where the broad negative dip is produced at  $R_m = 1$ , as demonstrated in Fig. 3. With an increase in  $R_m$ , the potential dip becomes sharp and shifts towards the mirror point, showing an increase of the depression depth. The maximum depth, however, is  $(1-3)T_{e1}/e$  in our range of  $R_m$  at any value of  $P_{20}/P_{10}$ .

In Fig. 4, a dependence of the potential shape on the argon-gas pressure is shown at  $R_m = 2.7$ . As the pressure is decreased, the potential slope becomes small in the discharge plasma and the potential drop is much localized around the potential depression, resulting in a more remark-

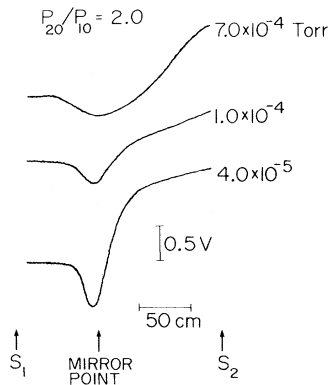


FIG. 4. Potential distributions at argon-gas pressures of  $7 \times 10^{-4}$  ( $9.5 \times 10^{-4}$ ),  $1.0 \times 10^{-4}$  ( $3.0 \times 10^{-4}$ ), and  $4.0 \times 10^{-5}$  ( $1.5 \times 10^{-4}$ ) Torr in the experimental region. The pressures near  $S_2$  are given by the values in the parentheses.  $R_m = 2.7$ .

able feature of the phenomenon. At the pressure of  $4.0 \times 10^{-5}$  Torr, the ion collision mean path is about 200 cm, and thus the collisional effects can be neglected. The measured shape of the potential profile reminds us of the double layers with the potential dip on the low-potential tail.

As described above, the potential of the plasma supplied from  $S_1$  is not fixed externally, but is determined by a contact with the plasma supplied from  $S_2$ , yielding the potential profile with the potential depression between the two plasmas. The phenomenon is enhanced at such a gas pressure where the collisions are neglected and there is no appreciable generation of fluctuations causing anomalous resistivity. Thus, Hultqvist's theory<sup>5</sup> for thermoelectric effect cannot be applied to this experiment. Under our potential configuration, both groups of electrons supplied from  $S_1$  and  $S_2$  are reflected by the potential decreasing towards the potential dip except for a small amount of high-energy tail electrons. Ions supplied from  $S_1$  are reflected by the potential slope between the dip position and  $S_2$ . On the other hand, ions supplied from  $S_2$  can pass through the potential dip towards  $S_1$ . The electric current due to these ions is compensated by the electric current due to the high-energy tail electrons, resulting in no net electric current passing through the plasma column. In fact, the tail electrons with energy of 4 eV are observed to pass through the dip towards  $S_1$ . Since the density is less than 1% of the bulk electrons in the discharge plasma, the energy transport [ $\propto$  density  $\times$  (energy)<sup>3/2</sup>] due to the tail electrons is negligibly small ( $\approx 4\%$ ). The plasma density decreases towards

the potential dip and the minimum appears at the same position as  $\varphi$ . The electron temperature increases slightly towards  $S_2$ , but an abrupt change is observed around the potential dip. The measured relation between the density and potential profiles is found to be consistent within an error of 20% with the prediction based on the Boltzmann relation.<sup>10</sup> In the presence of the magnetic bump, we must take into account the ion deceleration and reflection due to the magnetic mirror, which give rise to a change of the plasma density, resulting in the modification of the plasma potential. The density at the position of the maximum magnetic field is observed to decrease with an increase in  $R_m$ , being consistent with the localization of the potential depression at the magnetic bump.

In conclusion, the potential depression separates the two spatial regions with higher potential of the order of the corresponding electron temperature and isolates the two groups of electrons from each other, reducing thermal contact between the two plasmas. In the thermal-barrier variation of the tandem mirror,<sup>4</sup> this kind of thermal barrier has been expected to be formed by sloshing charged particles in a magnetic well.<sup>11</sup> Although our thermal barrier is localized at the mirror throat, the experiment shows an essential feature of thermal-barrier formation between two different plasmas. The result should correspond to a kind of the Bernstein-Greene-Kruskal solutions<sup>12</sup> of the Vlasov-Poisson equations including effects of magnetic mirror. Finally, it is to be noted that the potential depression observed is closely related to the negative potential dip formed on the low-potential tail of double layers.<sup>8</sup>

We acknowledge useful discussions with Dr. K. Saeki and Dr. M. Inutake. We are also indebted to T. Mieno, T. Kanazawa, and T. Haiji for their experimental support.

<sup>1</sup>P. Carlqvist, *Solar Phys.* **7**, 377 (1969); F. S. Mozar *et al.*, *Phys. Rev. Lett.* **38**, 292 (1977); S. D. Shawhan *et al.*, *J. Geophys. Res.* **83**, 1049 (1978).

<sup>2</sup>G. I. Dimov *et al.*, *Fiz. Plasmy* **2**, 597 (1976) [*Sov. J. Plasma Phys.* **2**, 326 (1976)]; T. K. Fowler and B. G. Logan, *Comments Plasma Phys. Controlled Fusion* **2**, 167 (1977).

<sup>3</sup>F. H. Coengen *et al.*, *Phys. Rev. Lett.* **44**, 1132 (1980); R. Breun *et al.*, *Phys. Rev. Lett.* **47**, 1833 (1981).

- <sup>4</sup>D. E. Baldwin and B. G. Logan, Phys. Rev. Lett. 43, 1318 (1979).
- <sup>5</sup>B. Hultqvist, Planet. Space Sci. 19, 749 (1971).
- <sup>6</sup>F. W. Perkins and Y. C. Sun, Phys. Rev. Lett. 46, 115 (1981); Y. Nakamura and R. L. Stenzel, in Proceedings of the Symposium on Plasma Double Layers, Risø, 1982, Risø National Laboratory Research Report No. Risø-R-472 (to be published).
- <sup>7</sup>P. Coakley and N. Hershkowitz, Phys. Fluids 22, 1171 (1979); P. Leung *et al.*, Phys. Fluids 23, 992 (1980); S. Iizuka *et al.*, Phys. Rev. Lett. 43, 1404 (1979); R. L. Stenzel *et al.*, Phys. Rev. Lett. 45, 1498 (1980).
- <sup>8</sup>N. Sato *et al.*, Phys. Rev. Lett. 46, 1330 (1981); S. Iizuka *et al.*, Phys. Rev. Lett. 48, 145 (1982).
- <sup>9</sup>S. C. Brown, *Basic Data of Plasma Physics* (MIT Press, Cambridge, Mass., 1966).
- <sup>10</sup>R. H. Cohen *et al.*, Nucl. Fusion 20, 1421 (1980).
- <sup>11</sup>J. Kesner, Nucl. Fusion 20, 557 (1980), and 21, 97 (1981).
- <sup>12</sup>Ira B. Bernstein, John M. Greene, and Martin D. Kruskal, Phys. Rev. 108, 546 (1957).